8/15/80

0 0 0 0 4 0 0 4 4 2

4
LBL-9443 c.1
Preprint

Lawrence Berkeley Laboratory
UNIVERSITY OF CALIFORNIA

Materials & Molecular Research Division

Submitted to the Journal of the American Ceramic Society

VAPOR PHASE HYDRATION OF SUBMICRON PARTICLES OF CaO

Dario Beruto, Alan W. Searcy, Luigi Barco, and Gabriele Belleri

June 1980

RECEIVED
LAWRENCE
BERKELEY LABORATORY

MAR 24 1981

For Reference

Not to be taken from this room

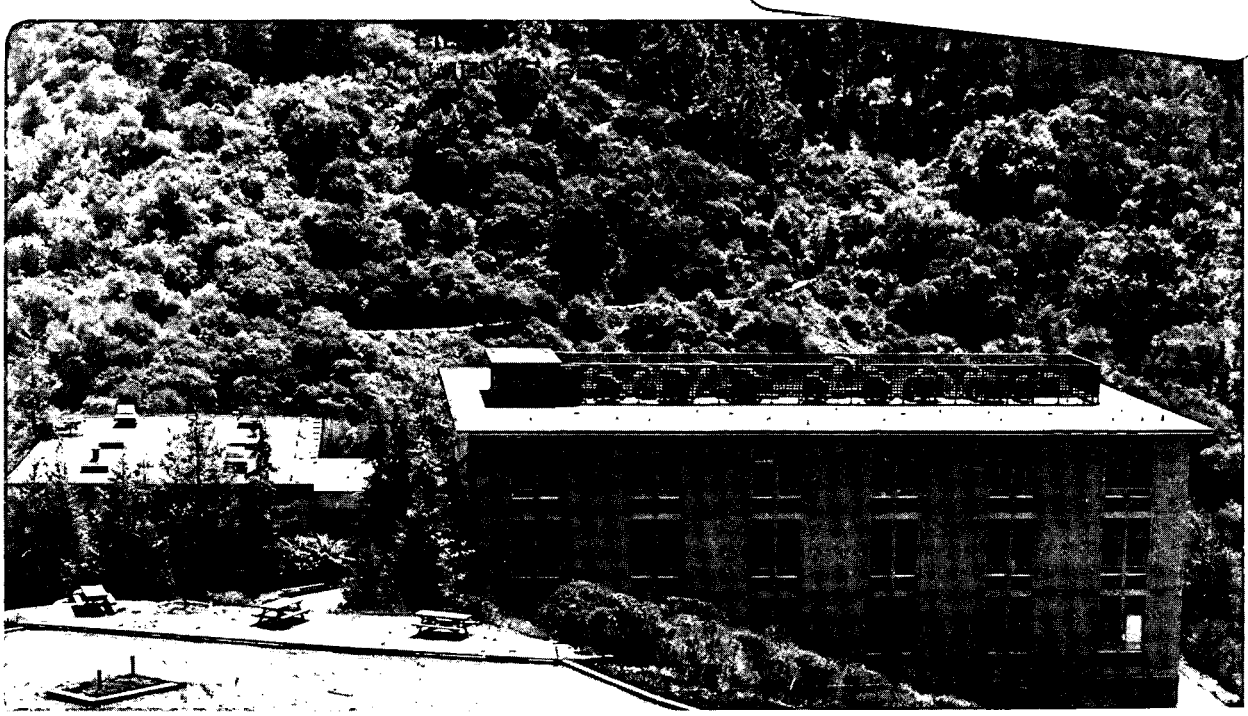

LBL-9443 c.1

4

Prepared for the U.S. Department of Energy under Contract W-7405-ENG-48

LEGAL NOTICE

This book was prepared as an account of work sponsored by an agency of the United States Government. Neither the United States Government nor any agency thereof, nor any of their employees, makes any warranty, express or implied, or assumes any legal liability or responsibility for the accuracy, completeness, or usefulness of any information, apparatus, product, or process disclosed, or represents that its use would not infringe privately owned rights. Reference herein to any specific commercial product, process, or service by trade name, trademark, manufacturer, or otherwise, does not necessarily constitute or imply its endorsement, recommendation, or favoring by the United States Government or any agency thereof. The views and opinions of authors expressed herein do not necessarily state or reflect those of the United States Government or any agency thereof.

DISCLAIMER

This document was prepared as an account of work sponsored by the United States Government. While this document is believed to contain correct information, neither the United States Government nor any agency thereof, nor the Regents of the University of California, nor any of their employees, makes any warranty, express or implied, or assumes any legal responsibility for the accuracy, completeness, or usefulness of any information, apparatus, product, or process disclosed, or represents that its use would not infringe privately owned rights. Reference herein to any specific commercial product, process, or service by its trade name, trademark, manufacturer, or otherwise, does not necessarily constitute or imply its endorsement, recommendation, or favoring by the United States Government or any agency thereof, or the Regents of the University of California. The views and opinions of authors expressed herein do not necessarily state or reflect those of the United States Government or any agency thereof or the Regents of the University of California.

0 0 0 0 5 4 0 5 4 4 3

VAPOR PHASE HYDRATION OF SUBMICRON PARTICLES OF CaO

Dario Beruto,*+ Alan W. Searcy,+ Luigi Barco,*
and Gabriele Belleri*

ABSTRACT

Reaction of water vapor at 25°C with CaO powder of either high or low surface area yields $Ca(OH)_2$ with broad XRD peaks. Relative rates of reaction of these hydroxides with CO_2 at 250°C depend mainly on the sample surface areas per unit weight. SEM observations show that the exterior shapes of porous 1 to 30 μm particles of CaO formed by decomposition in vacuum of $CaCO_3$ (called sr-CaO) or $Ca(OH)_2$ (called h-CaO) are little changed when they are converted to $Ca(OH)_2$, except for surface roughening, which increases with time of exposure to water vapor. N_2 adsorption-desorption isotherms of h-CaO, sr-CaO, and of their hydration products are used to calculate the average particle expansion, the probable pore shapes, and the changes in pore size distributions that accompany the reaction. These data show that the reaction causes expansion perpendicular to interior surfaces of the porous powder particles. A possible mechanism is suggested. Both h-CaO and sr-CaO dissolve in liquid water to yield $Ca(OH)_2$ by subsequent precipitation.

I. INTRODUCTION

When either $CaCO_3$ [1-3] or $Ca(OH)_2$ [3] powder is decomposed in vacuum, CaO is produced as particles that have almost the same exterior dimensions as the particles of the parent solid. Figures 1-3 illustrate the relations for $CaCO_3$ decomposition and subsequent hydration. But the CaO powder particles are highly porous aggregates of CaO crystallites, which react very rapidly with water vapor.

Orientation of the $Ca(OH)_2$ relative to the CaO crystallites of these porous aggregates would be difficult to obtain by diffraction techniques because the crystallites have dimensions of the order of only 10 nm (100 Å).[3] But in this paper N_2 adsorption-desorption isotherms are used to show that the predominant $Ca(OH)_2$ growth is normal to the surfaces of these crystallites. The paper also reports particle morphologies as revealed by observations with a scanning electron microscope (SEM), crystallinities as measured by XRD line broadening, and surface areas of the $Ca(OH)_2$ produced by reaction of porous and nonporous CaO powders with water vapor.

II. EXPERIMENTAL

Spectroscopic analyses of the materials that served as sources for the porous CaO used in the hydration studies are reported in Table I. Surface areas and XRD line broadening

measurements for CaO samples are reported in Table II. In this table and in the text, the CaO produced by decomposition of $CaCO_3$ powder in vacuum is called sr-CaO and the CaO produced by decomposition of $Ca(OH)_2$ in vacuum is called h-CaO. CaO produced by decomposing large crystals of $CaCO_3$ is called sc-CaO. It has a slightly higher surface area and a higher degree of crystallinity, as measured by XRD peak area divided by peak height, than does sr-CaO.[3]

CaO samples that weighed 27 mg were used in all of the hydration studies. The water vapor pressure was measured with an MKS baratron single-sided absolute sensor head. The uptake of water vapor was followed gravimetrically with a Sartorius microbalance in a system, which was connected with a large reservoir of water that was kept at the temperature that gave the desired pressure of water vapor. The h-CaO samples were prepared by decomposing $Ca(OH)_2$ of two kinds, irregular particles and block-like particles, at 300°C in the apparatus. Because preparation of sr-CaO or sc-CaO required decomposition of $CaCO_3$ at ~510°C, a higher temperature than practical in the pyrex tube of the hydration system, these materials were prepared in a Netzsch thermobalance and were transferred to the adsorption-apparatus as quickly as possible. During transfer, the sr-CaO samples gained 14 to 18% of the theoretical weight required for conversion to $Ca(OH)_2$ because of reaction with water vapor in air.[3] The $Ca(OH)_2$ formed during transfer was decomposed in

vacuum at 300°C in the hydration apparatus. One sample of sr-CaO was prepared directly in a new quartz apparatus and its surface area was measured without exposure to the atmosphere. The surface area was 70 m^2/g in reasonable agreement with values reported below. The partial hydration and dehydration, therefore, did not seriously influence our results.

The hydration reaction temperature was held constant at 25°C by a reservoir of water that surrounded the Pyrex tube in which the samples were suspended. The system was evacuated to 10^{-4} Pa, and then water at the selected pressure was admitted to the apparatus. The water vapor pressure could be held constant to ±10 Pa. All runs were continued to 100% of the theoretical gain. In order to avoid changes in surface areas that are known to occur with time after reaction was completed,[4] the system was immediately evacuated. A constant weight was reached when the samples had lost 4 to 6% of their water content. Perhaps this water was adsorbed in the interior particle surfaces so that conversion of CaO to $Ca(OH)_2$ was only ~95% complete.

To study separately the effect on the morphology of the hydroxides of continued exposure to water vapor, a set of samples was held in water vapor for times of 10 to 40 hours after hydration reached 100%.

The dried $Ca(OH)_2$ samples were cooled under vacuum in the same apparatus to 78K for measurement of adsorption-desorption

isotherms with N_2 gas volume changes and from changes in weight of the sample. The results agree at low relative pressures, but the volumetric method is less accurate at high relative pressures of N_2. Consequently, the thermogravimetric method was used for determinations reported in this paper.

Samples of $Ca(OH)_2$ prepared from CaO of different porosity and of a range of exposures to water vapor were examined with an SEM after the isotherm measurements. Samples were prepared for the SEM studies by dropping them on a gold-coated surface, and coating them with a layer of gold 30 nm thick. The time of exposure to water vapor during transfer is too short to influence particle morphology at a scale observable by SEM. XRD studies were made on powders packed in an Al holder using a Philips powder diffractometer with a proportional detector and Co Kα radiation.

The relative reactivities of the $Ca(OH)_2$ samples toward CO_2 at 600 Pa pressure were measured at a constant temperature of 250°C and also with constant 2°C/min heating to 300°C. For these studies, samples were suspended in an alumina crucible from a Netzsch thermobalance.

III. RESULTS

The hydration of CaO by liquid water, which is an important reaction in the setting of cements, has been extensively studied,[4-6] but apparently has not been studied with such high

surface area forms of CaO as used in the present investigation. Both h-CaO and sr-CaO react more rapidly and more exothermally with liquid water than does CaO of low surface area. SEM pictures show that the reaction produces well-crystallized $Ca(OH)_2$ particles on the surfaces of the original porous CaO particles and on the walls of the reaction vessel. The line broadening of the major XRD peak of this $Ca(OH)_2$, as measured by the ratio of the area of the peak to the peak height is low (Table III, Line 1), as is the ratio for commercial $Ca(OH)_2$ (Table III, Line 2) of relatively low 6 m^2/g surface area. The path of reaction of h-CaO and sr-CaO with liquid water must be the same as the path for reaction of CaO powders of low surface area.[6] The CaO dissolves in the water and $Ca(OH)_2$ precipitates from the solution.

When water vapor was used as the hydrating agent, sr-CaO and h-CaO were more than 50% converted to $Ca(OH)_2$ in less than two minutes. Reaction of low surface area samples of CaO proceeded at much lower rates. Hydration of either high or low surface area CaO powders with water vapor always yielded a $Ca(OH)_2$ which had broad peaks, indicating the $Ca(OH)_2$ to have small crystallite sizes and/or high internal strains (Table III).

The morphologies of the $Ca(OH)_2$ particles that result from reaction of water vapor with sr-CaO (called sr-$Ca(OH)_2$) or with h-CaO (called h-$Ca(OH)_2$) suggest that the reaction path is very different from that when liquid water is used (Fig. 4). Just

as the porous particles of sr-CaO and h-CaO retain almost the same exterior dimensions as do the $CaCO_3$ and $Ca(OH)_2$ parent particles, so do sr-$Ca(OH)_2$ and h-$Ca(OH)_2$ particles retain almost these same exterior dimensions (Fig. 3). This observation implies that the reaction proceeds primarily at internal surfaces of the CaO crystallites, which form the porous 1 to 30 μm particles that are observed by SEM. The particles of sr-CaO are formed of aggregates of CaO needles that have diameters of ~10 nm.[7] From N_2 adsorption-desorption isotherms, the particles of h-CaO are inferred to be composed of sheets of CaO,[3] like MgO produced by decomposition of $Mg(OH)_2$.[8]

Close examination of the SEM photographs shows that sr-$Ca(OH)_2$, like sr-CaO,[3] has somewhat less sharp edges than the $CaCO_3$ from which sr-CaO is produced. Some larger sr-$Ca(OH)_2$ particles are cracked (Fig. 5). Crack formation is favored by reaction with water at higher partial pressures, perhaps because the greater reductions in porosity, which are revealed by the adsorption isotherms, introduce higher levels of strain.

The sr-$Ca(OH)_2$, if exposed to water vapor at ~500 Pa pressure 10 hours, showed no significant surface roughening; but when the water vapor pressure was increased from 500 to 3000 Pa and the exposure time was increased to 35 to 40 hours, scales could be observed. The integral breadth of the major peak of the XRD pattern of these samples was less (15×10^{-3} rad) than for the

corresponding hydroxide listed in Table III. A repeated cycle of vacuum decomposition at 300°C and rehydration followed by 36 to 40 hours exposure to water vapor caused a significant change in morphology. As Fig. 6 shows, at the highest water partial pressures and times the scales became more clearly defined and more definitely aligned into ridges parallel with sides of the original particles. The h-$Ca(OH)_2$ particles formed at higher H_2O vapor pressures had similar features.

Table IV summarizes the results of exposure of $Ca(OH)_2$ prepared from high and low porosity CaO powders to ~700 Pa pressure of CO_2 at 290°C. These poorly crystalline forms of $Ca(OH)_2$ all react rapidly with CO_2. The sr-$Ca(OH)_2$ reacts most rapidly, but the rates per unit area of surface are approximately the same. The dynamic measurements were consistent with the isothermal measurements.

The adsorption isotherms of sr-$Ca(OH)_2$ were all of Type IV.[9] The steeply sloping loops are consistent with De Boer's predictions[10] for pores of cylindrical symmetry (Fig. 7). Cylindrical symmetry would result if the needles that form sr-CaO[7] align in bundles with their axes parallel and hydrate to particles of similar shapes. The t-method[11-12] was applied and the relationship between the statistical thickness t of the adsorbed gas and the relative pressure P/Po was evaluated using the value of a C-constant estimated from BET data.[15] Figure 8 shows the

results. All plots showed upward curvature, which is also consistent with the conclusion that the pores have curved walls.[16]

Adsorption isotherms for h-$Ca(OH)_2$ were Brunauer's classification Type II,[9] like the parent h-CaO (Fig. 9). Downward sloping t-method plots and the sloping shapes of the adsorption and desorption isotherms are of a kind which De Boer[10] predicts for capillary systems of planar symmetry. Planar symmetry is consistent with the interpretation that (a) the h-CaO is produced by escape of H_2O by preferential diffusion in the plane normal to the crystallographic c-axis, and (b) the capillaries formed when h-CaO reacts with water vapor retain this planar symmetry.

Figure 10 shows the succession of adsorption-desorption isotherms that result for the hydroxides of the sequence sr-CaO $\rightarrow$ $Ca(OH)_2$ $\rightarrow$ CaO $\rightarrow$ $Ca(OH)_2$ $\rightarrow$ CaO $\rightarrow$ $Ca(OH)_2$ when 2400 Pa $H_2O_{(g)}$ pressure was used for hydration. The hydration-dehydration cycles decrease the pore volume and change the isotherm shape. If the partial hydration during transfer of sr-CaO had been avoided, the sr-$Ca(OH)_2$ isotherms would probably have shown essentially the shapes reported, but with slightly higher intercepts on the vertical axis. The Type IV isotherm of the first hydroxide is seen to be transformed in the direction of isotherms characteristic of slit-shaped pores. Variations in N_2 adsorption with N_2 layer thickness measured by the t-method[11,12] indicated the same trend. Unless the product sr-$Ca(OH)_2$ was aged in water

vapor for a period much longer than the ~1/3 hour required for the cycling, features like those of Fig. 6 were not apparent.

It was recently shown that the average porosities of h-CaO and sr-CaO particles can be calculated from the volume of N_2 that they absorb when the N_2 pressure is infinitesimally below the equilibrium vapor pressure of N_2 at 78K.[3] By this means, the porosity of sr-CaO was found to be 41.5 ± 5%, and that of h-CaO to be 36 ± 5%, compared to theoretical porosities of ~55% and ~50% calculated from the molar volumes of $CaCO_3$, $Ca(OH)_2$, and CaO on the assumption that the initial $CaCO_3$ and $Ca(OH)_2$ particle dimensions are exactly retained by the porous aggregates of CaO formed by the decomposition reactions.

The discrepancy between the measured and theoretical porosities indicates that the porous particles of h-CaO and sr-CaO average about 5% smaller in linear dimensions than their parent $Ca(OH)_2$ and $CaCO_3$ particles. The same approach can be used to demonstrate that the reaction of sr-CaO or h-CaO with water vapor produces an increase in the average size of the porous particles that are observed by SEM. The theoretical porosities reported for the $Ca(OH)_2$ from sr-CaO (Table V) were calculated from the difference in molar volumes between $CaCO_3$ and $Ca(OH)_2$. The volume expansions quoted in column 4 are relative to the original $CaCO_3$ or $Ca(OH)_2$ particles. Hydration of sr-CaO at 120 Pa, for example, resulted in $Ca(OH)_2$ particles with linear dimensions that averaged 4 to 5% greater than the $CaCO_3$ from which the sr-CaO

particles were produced, even though the sr-CaO particles were 4 to 5% smaller in linear dimensions than the $CaCO_3$ particles.

In conformity with the above analysis, we calculated the pore size distribution assuming an ink bottle with cylindrical body for sr-$Ca(OH)_2$ samples and open slit-shaped pores for the h-$Ca(OH)_2$. These assumed shapes are consistent with the pore symmetries deduced for sr-$Ca(OH)_2$ and h-$Ca(OH)_2$ and with the findings that these assumed shapes give cumulative surface areas that are in reasonable agreement with the surface areas measured by the BET method (Table IV). These assumptions influence the shapes of calculated pore size distribution curves, but not the trends of changes in pore volumes and pore size distributions calculated when sr-CaO or h-CaO is hydrated.

Figure 11 shows the pore size distributions calculated for the $Ca(OH)_2$ produced from reaction of sr-CaO with water vapor at various pressures. It is noteworthy that the reduced total porosity for samples prepared at relatively high partial pressures of water is a consequence more of reducing the number of pores than of reducing their average dimensions.

Figure 12 compares the porosity of h-CaO to porosities of $Ca(OH)_2$ produced by reacting h-CaO with water vapor at two different partial pressures. Again, the lower porosity in the sample prepared under a high partial pressure of water appears to be

a consequence of a smaller number of pores rather than of a reduction in average pore cross-sections.

DISCUSSION

Because the reaction of porous CaO particles with water vapor proceeds rapidly at only 25°C, the reaction path might be thought to be capillary condensation of water followed by solution of CaO and precipitation of $Ca(OH)_2$ in the capillaries. But the reactions of both sr-CaO and h-CaO proceed readily when the water vapor pressure is 500 Pa and the saturated vapor pressure of water is about 3×10^3 Pa. At this low relative pressure the Kelvin equation predicts that capillary condensation would occur only in pores <1 nm in radius,[13] but the measured pore radii in sr-CaO are all >1 nm.

The probable path for $Ca(OH)_2$ decomposition and a possible path of reaction of porous CaO particles with water vapor can be described by reference to the crystal structures of $Ca(OH)_2$ and CaO (Fig. 3). $Ca(OH)_2$ has a highly anisotropic layer structure. Partial decomposition of $Ca(OH)_2$ at low water pressures yields CaO in which the (111) planes of the NaCl-type unit cells of CaO tend toward preferential alignment with the (001) hexagonal basal planes of the parent $Ca(OH)_2$.[14] For $Mg(OH)_2$, which is structurally similar to $Ca(OH)_2$,[6] decomposition is known to occur by diffusion of H_2O from the lattice in the plane

perpendicular to the crystallographic c-axis.[8] The MgO is left as parallel polycrystalline sheets. Decomposition of $Ca(OH)_2$ by a similar reaction path would yield polycrystalline sheets of CaO crystallites with the observed tendency for (111) planes of CaO to be parallel to (001) planes of the parent $Ca(OH)_2$.

For pores to close as h-$Ca(OH)_2$ grows by reaction of water with h-CaO requires that water be transported into the solid CaO and that some CaO be transported outward from the original h-CaO pore surface. In the absence of a liquid phase solution-precipitation process, rapid enough diffusion of Ca^{++} and $O^{=}$ over even a few lattice spacings to account for the observed reaction rate at room temperature seems highly improbable. A reaction path that combines solid-state diffusion of H_2O and strain-induced movement of product $Ca(OH)_2$ to refill most of the pore volume of the h-CaO or sr-CaO particles is suggested below. The analysis developed for h-CaO is consistent with observations for sr-CaO and for nonporous CaO powders.

NaCl-type crystals do not have preferred directions of diffusion like those of the layer $M(OH)_2$ solids. The recombination of outer $O^{=}$ ion layers of water could occur by diffusion of H_2O into the CaO crystallites along the close-packed $O^{=}$(111) planes that are oriented most nearly normal to the slit-shaped pores that provide access of the water vapor. These $O^{=}$ planes of CaO would then become pairs of OH^{-}(001) planes of

$Ca(OH)_2$. But the conversion of $O^=$ planes of CaO to 2 OH^- planes of $Ca(OH)_2$ requires expansion in the direction normal to these planes by a factor of 4.91/2.78 ≈ 1.8 (see Fig. 11). Unless samples are held in high partial pressures of water vapor for long periods of time, the only SEM evidence that this large, anisotropic expansion has occurred is the occasional cracks that develop in the larger particles (Fig. 5). The interesting question is how this large anisotropic expansion is accommodated within porous particles of nearly fixed external dimensions.

The N_2 isotherms suggest an explanation. If no other process occurred to counter the effect of diffusion of H_2O into the h-CaO, the expected effect would be a great lengthening of the surface layers of each CaO sheet and only a small increase in sheet thickness. The expected result, if the reaction were carried to completion, would be a pore size distribution curve with a maximum value of $\Delta V/\Delta d$ greater than that shown by h-CaO, and with that maximum occurring at a pore width a little smaller than the width, ~2.7 nm, found for h-CaO (Fig. 11). But lengthening of the sheets as $Ca(OH)_2$ formation occurred would be blocked by impingement of the edges of most sheets against the faces of other sheets that make up each porous particle. Perhaps this restraint causes the expanded outer layers of the sheets (that part converted to $Ca(OH)_2$) to be extruded by sheer forces through the original surface.

The water released on heating to 100°C suggests that, at the time that the quantity of water theoretically sufficient to convert the porous CaO particles to $Ca(OH)_2$ has been adsorbed, conversion of CaO to $Ca(OH)_2$ is only ~95% complete, and ~5% water is adsorbed on the interior particle surfaces. Water may rapidly penetrate the $Ca(OH)_2$ grain boundaries to reach unreacted CaO below the $Ca(OH)_2$ layer, and water at these grain boundaries might reduce the energy necessary for the hypothesized shearing process.

The absence of pores of dimensions smaller than critical dimensions of the order of ~2 nm in sr-CaO,[2], sr-$Ca(OH)_2$ (Fig. 11), h-CaO, and h-$Ca(OH)_2$ (Fig. 12), suggests that such small pores are highly unstable and are rapidly eliminated. Pores of such small dimensions have not been the subject of conventional sintering studies.

ACKNOWLEDGMENT

Anthony G. Evans and Giorgio Spinolo provided helpful services. This work was supported by the Division of Materials Sciences, Office of Basic Energy Sciences, U.S. Department of Energy under contract No. W-7405-Eng-48 and by the Italy-U.S. Exchange Program of the Consiglio Nazionale Delle Ricerche and the National Science Foundation.

FOOTNOTES

*Laboratorio di Chimica Facolta di Ingegneria Universita di Genova, Italy.

+Materials and Molecular Research Division, Lawrence Berkeley Laboratory and Department of Materials Science and Mineral Engineering, University of California, Berkeley, U.S.A.

1. D. Beruto and A.W. Searcy, Calcium oxides of high reactivity. Nature 263, 221-222 (1976).
2. J. Ewing, D. Beruto, and A.W. Searcy, The nature of CaO produced by calcite powder decomposition in vacuum and in CO_2. J. Am. Ceram. Soc. 62, 581-584 (1979).
3. D. Beruto, A.W. Searcy, L. Barco, and G. Spinolo, Characterization of the porous CaO particles formed by decomposition of $CaCO_3$ and $Ca(OH)_2$ in vacuum, J. Am. Ceram. Soc., in press.
4. D.R. Glasson, Reactivity of lime and related oxides. II: Sorption of water vapor on calcium oxide. J. Appl. Chem. 8, 798-803 (1958).
5. V.S. Ramachandran, P.J. Sereda, and R.F. Feldman, Mechanism of hydration of calcium oxide. Nature 201, 288-289 (1964).
6. H.R. Oswald and R. Asper, in Preparation and Crystal Growth of Materials with Layered Structures, edited by R.M.A. Leith (D. Reidel Publishing Co., Dordrecth, Holland, 1977), pp. 71-140.

7. K.M. Towe, Ultrastructure of calcite decomposition in vacuo, Nature 274, 239-240 (1978).

8. R.S. Gordon and W.D. Kingery, Thermal decomposition of brucite. II: Kinetics of decomposition in vacuum. J. Am. Ceram. Soc., 50, 8-14 (1967).

9. S. Brunauer, The Adsorption of Gases and Vapors (Oxford Press, New York, 1943).

10. J.H. DeBoer, The Structure and Properties of Porous Materials, edited by D.H. Everett and F.S. Stone (Butterworth, Colston Papers, London, 1958), Vol. 10.

11. J.H. DeBoer, B.G. Linsen, and T.J. Osinga, Studies on pore systems in catalyst VI: The universal t-curve. J. Catalysis 4, 643-648 (1965).

12. B.C. Lippens, B.G. Linsen, and J.H. DeBoer, Studies on pore systems in catalysts I: The adsorption of nitrogen, apparatus, and calculation. J. Catalysis 3, 32-39 (1964).

13. R. Defay, I. Prigogine, A. Bellemans, and D.H. Everett, Surface Tension and Adsorption (J.H. Wiley and Sons, New York, 1966), p. 221.

14. N. Datta, S. Chatterji, J.W. Jeffery, and A.L. McKay, On the oriented transformation of $Ca(OH)_2$ to CaO. Min. Mag. 37, 250-252 (1959).

15. A. Lecloux, J.P. Pirard, The importance of standard isotherms in the analysis of adsorption isotherms for determining the porous texture of solids. J. of Colloid. Interface Science 70, 265-281 (1979).

16. J.C.P. Broekhoff and J.H. DeBoer, The surface area in intermediate pores, in Surface Area Determination, edited by D.H. Everett and R.H. Ottewill (Butterworths, London, 1969), p. 97.

Table I. Spectrographic Analysis of Starting Materials

Calcium Carbonate Powders

Impurity	Percent	Impurity	Percent
(NH_4)	0.003	Pb	0.0005
Ba	0.005	Na	0.1
(Cl)	0.005	K	0.01
Fe	0.002	(SO_4)	0.005
(NO_3)	0.1		

Calcium hydroxide powders

$CaCO_3$	3	(Cl)	0.001
(NO_3)	0.01	(SO_4)	0.005
Pb	0.001	Al	0.001
Mg	0.5	Fe	0.001
Ba	0.01	K	0.01
Na	0.1	Sr	0.1
Cu	0.0005	Zn	0.002

Table II. Surface Areas and Crystallinity of CaO from Various Sources

Material	Source of Material	Specific surface (m^2/g)	Integral breadth of major x-ray diffraction peak (rad. x 10^3)*
CaO	Decomposition $CaCO_3$ 3-10 μm powder, air 900°C	2	-
sr-CaO	Decomposition same $CaCO_3$ powder in vacuum, 500°C	78-81	9.8
CaO	Decomposition $Ca(OH)_2$ 6-10 μm powders in dry N_2, 400°C	2-3	5.5
h-CaO	Decomposition same $Ca(OH)_2$ powder in vacuum, 350°C (block-like particles)	133	13.1
h-CaO	Decomposition $Ca(OH)_2$ 1-10 μm powders in vacuum, 300-390°C (irregular particles)	110	≈15.5
sc-CaO	Decomposition $CaCO_3$ single crystal in vacuum, 580°C (.35x .5x .14(cm^3))	89	7.4
CaO	Commercial powder 10 μm particles		6.5

*The integral breadth is the ratio of the area of the peak to the peak height.

Table III. Surface Areas and Crystallinities of $Ca(OH)_2$

Material	Source of material	Specific surface S_{BET} (m^2/g)	Integral breadth of major x-ray diffraction peak of parent CaO (200) (Rad. x 10^3)	Integral breadth of major x-ray $Ca(OH)_2$ diffraction peak $(101)_H$ (Rad. x 10^3)
$Ca(OH)_2$	Hydration sr-CaO with liquid water, room temperature	16	9.83	~4
	Commercial block-shaped particles	6.6	–	4.3
	Hydration sr-CaO, 500 Pa, 25°C	39.8	9.83	22.9
	Hydration h-CaO granular block particles, 500 Pa, 25°C	16.5	13.1	23.4
	Hydration h-CaO irregular shape particles, 500 Pa, 25°C	28	~15.5	~23
	Hydration sc-CaO, 500 Pa, 25°C	38.8	7.4	17.7
$Ca(OH)_2$ - CaO	Hydration low specific surface CaO from $CaCO_3$ 500 Pa, 25°C	3	~6	14.1
	Hydration low specific surface CaO from $Ca(OH)_2$, 500 Pa 25°C	~3	5.5	15.4
$Ca(OH)_2$	Hydration commercial CaO, 500-3000 Pa, 25°C	6	~6	13.3

Table IV. Results of Exposure of $Ca(OH)_2$ to ~700 Pa Pressure of CO_2 for Six Hours

Materials	Source	Initial weight W_0(mg)	Final degree of conversion %	Average rate of reaction (%/h)	(%/h(m^2g^{-1}/)
sr-$Ca(OH)_2$	sr-CaO	25.6	~94	15.6	15.3
h-$Ca(OH)_2$	h-CaO granular block particles	17.3	~30	5	17.5
$Ca(OH)_2$	commercial granular block particles	16.9	~18	3	18.6

*Weight and specific surface values are relevant to the initial particles of $Ca(OH)_2$.

Table V. Surface Areas and Volumes of $Ca(OH)_2$

Material	Hydration conditions P_{H_2O}* (Pa)	Specific surface (m^2/g) S_{BET}	S_t	Cumulative surface (m^2/g) ink bottle	slit shape	Volume adsorbed at saturation point (cm^3 STP/g)	Cumulative volume (cm^3 STP/g)
$Ca(OH)_2$ from sr-CaO	120	44.8	43.0	46.8	59.5	78.3	75
	550	39.8	38.1	39.9	55.3	67.5	64
	1100	31.9	30.5	33.2	49.5	57.4	55
	1700	27.0	26.4	28.3	43.6	52.3	50
	2200	23.3	22.5	22.1	37.4	48.9	45
$Ca(OH)_2$ from h-CaO granular block particles	500	16.5	15.9	13.5	18.0	37.6	36.2
	2000	12.1	11.8	7.5	10.0	27.48	23
$Ca(OH)_2$ from sc-CaO	500	38.8	35.6	38.1	-	45	42.7

*Hydration temperature was 25°C for all experiments.

**Cumulative volume (V_{Cum}) is the volume corresponding to the pore size distribution that gave the cumulative surface (S_{Cum}) value nearest to S_{BET} and S_t.

Table VI. Comparison of Experimental and Theoretical Porosities.

Material	Water vapor pressure* (Pa)	Theoretical porosity %	Experimental porosity %	Average particle volume expansion %	Average linear expansion %
sr-$Ca(OH)_2$	120	9.06	27.3	13.7	~4.5
	550	9.06	23.5	10.4	-
	1100	9.06	19.9	7.16	-
	1700	9.06	18.1	5.5	-
	2200	9.06	17.0	4.6	-
h-$Ca(OH)_2$	500	0	12.9	5.8	-
	2000	0	9.6	4.3	~1.4

*All hydrations were carried out at 25°C.

FIGURE CAPTIONS

Figure 1. SEM photograph (10,000X) of $CaCO_3$ particles.

Figure 2. SEM photograph (10,000X) of sr-CaO particles produced by decomposing $CaCO_3$ particles in vacuo.

Figure 3. SEM photograph (20,000X) of $Ca(OH)_2$ produced by reaction of water vapor (pressure, 500 Pa; temperature, 25°C) with CaO from decomposition of $CaCO_3$ in vacuo. Shapes are essentially those of the original rhombohedral $CaCO_3$ particles and of sr-CaO.

Figure 4. SEM photograph (20,000X) of $Ca(OH)_2$ produced by reaction of liquid water with sr-CaO.

Figure 5. SEM photograph of cracked $Ca(OH)_2$ particles produced from reaction of sr-CaO with water vapor at ~1700 Pa (20,000X).

Figure 6. Particles of $Ca(OH)_2$ formed from the sequence sr-CaO → $Ca(OH)_2$ → h-CaO → $Ca(OH)_2$ → h-CaO → $Ca(OH)_2$ showing rough parallel ridges (20,000X).

Figure 7. N_2 adsorption-desorption isotherms at 78.15°K for $Ca(OH)_2$ prepared from sr-CaO at H_2O pressures of 120 Pa (curve A), 550 Pa (curve B), 1100 Pa (curve C), 1700 Pa (curve D), and 2200 Pa (curve E).

Figure 8. Volume of N_2 adsorbed as a function of the statistical thickness for $Ca(OH)_2$ prepared from sr-CaO at H_2O pressures of 130 Pa (curve A), 550 Pa (curve B), 1100 Pa (curve C), 1700 Pa (curve D), and 2200 Pa (curve E).

Figure 9. N_2 isotherms at 78K for $Ca(OH)_2$ prepared from h-CaO at H_2O pressures of 500 Pa (curve F) and 2000 Pa (curve G).

Figure 10. N_2 isotherms of 78.15K for the hydroxides of the sequence: sr-CaO → $Ca(OH)_2$ (curve H) → h-CaO → $Ca(OH)_2$ → (curve I) → h-CaO → $Ca(OH)_2$ (curve L).

Figure 11. Pore size distributions in $Ca(OH)_2$ produced by reaction of sr-CaO with water vapor at 120 Pa (curve A), 550 Pa (curve B), 1100 Pa (curve C), 1700 Pa (curve D), and 2200 Pa (curve E).

Figure 12. Pore size distributions in h-CaO (curve I) and in $Ca(OH)_2$ produced by reaction of h-CaO with H_2O vapor at 500 Pa pressure (curve II) and 15 torr pressure (curve III).

Figure 13. Perspective drawing of $Ca(OH)_2$ structure (left) and CaO structure (right). The shaded horizontal planes have close-packed Ca^{++} ions. The reaction causes only small changes in spacings within these close-packed planes 0.359 nm → 0.340 nm, but causes large changes in the direction normal to these planes (0.491 nm → 0.278 nm).

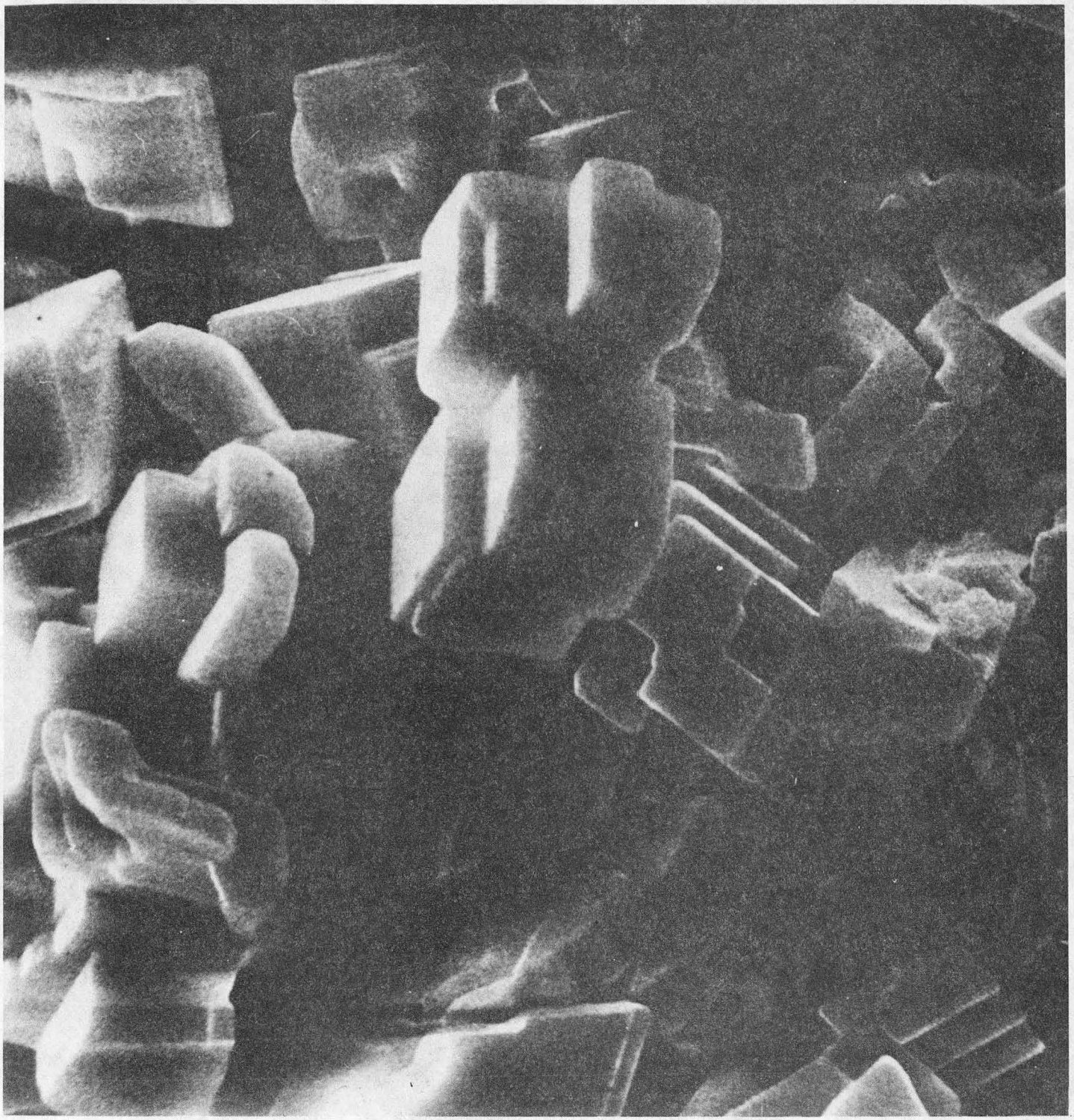

XBB766 5106

Fig. 1

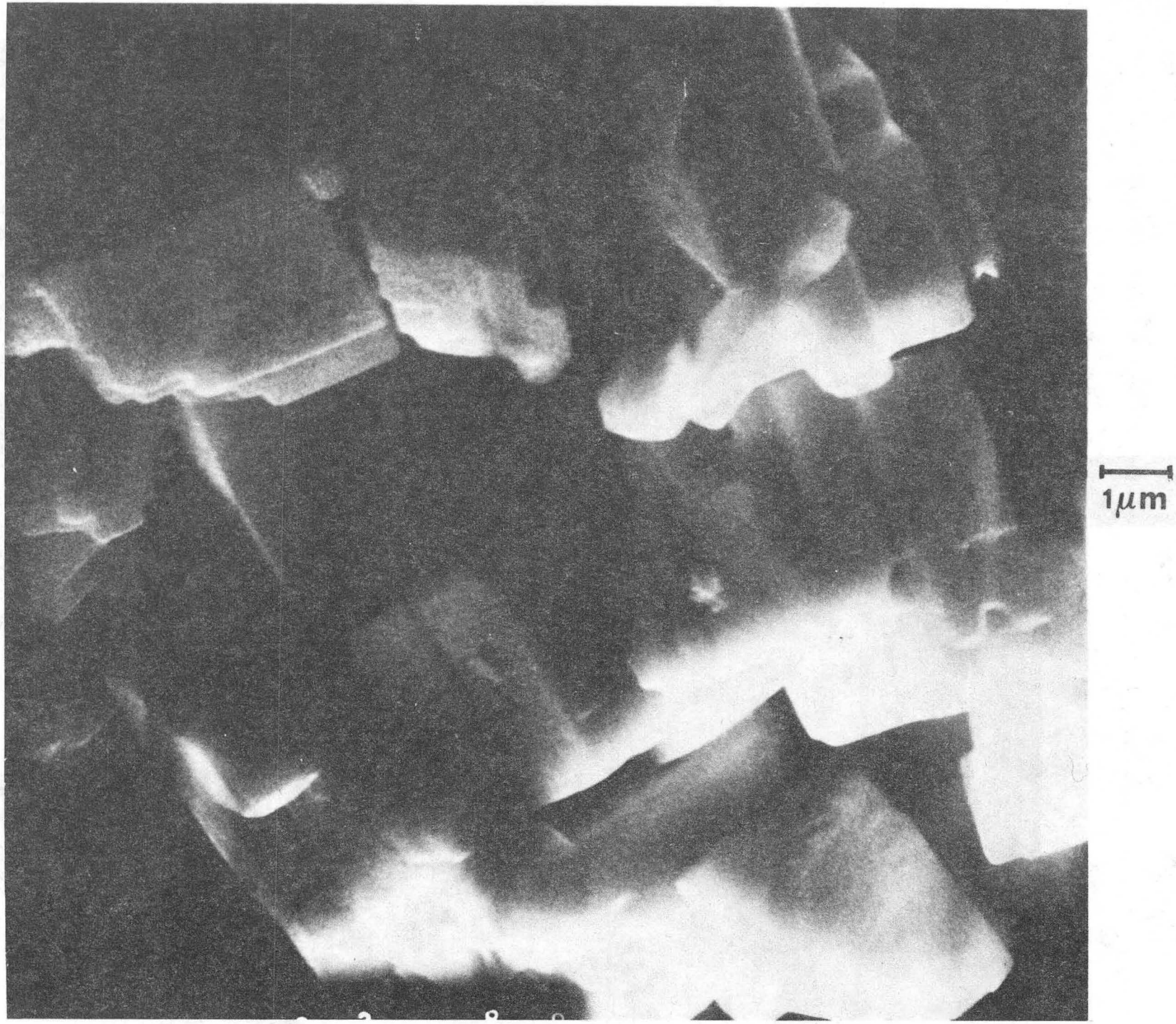

Fig. 2

XBB766 5108

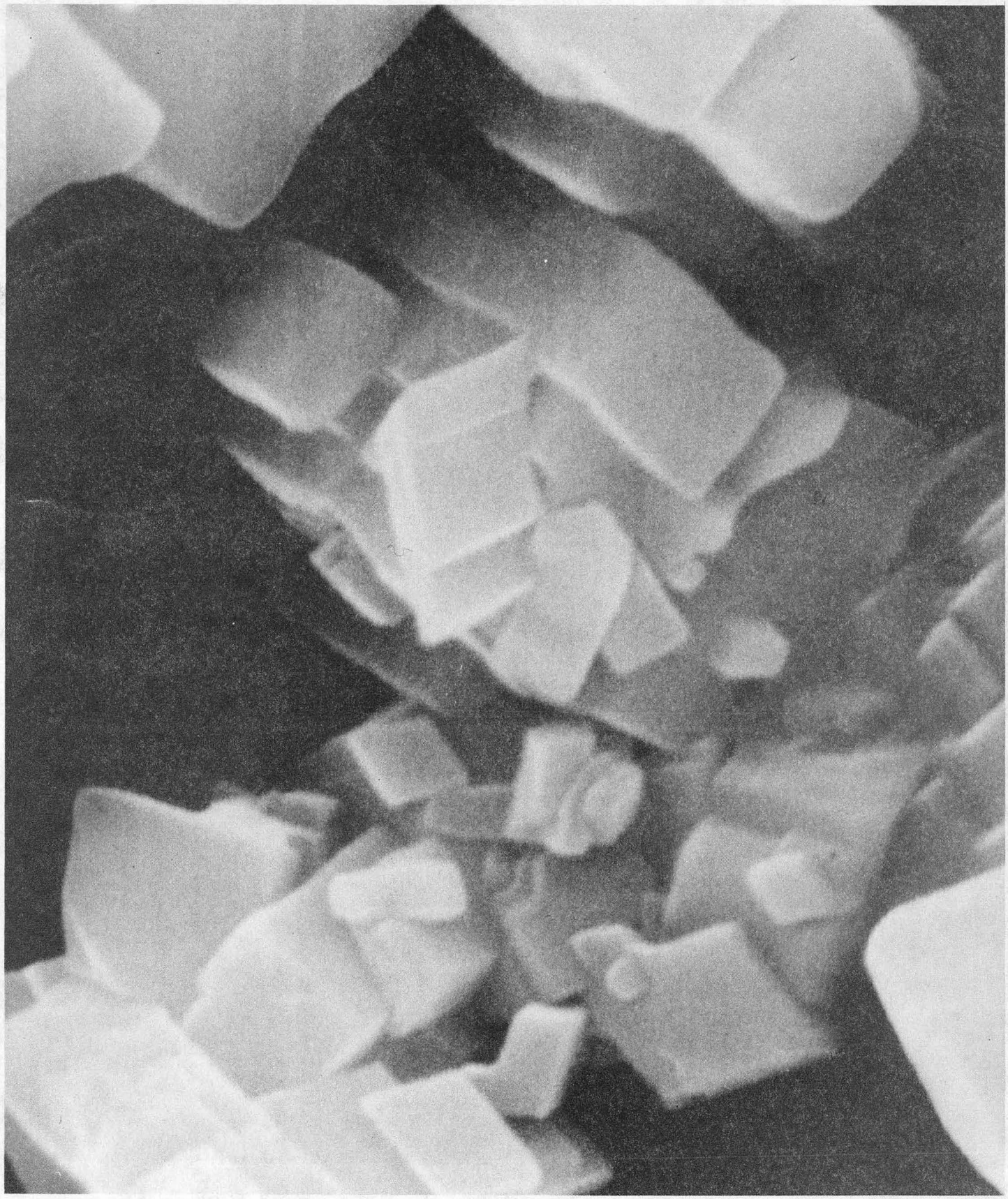

XBB796-8299

Fig. 3

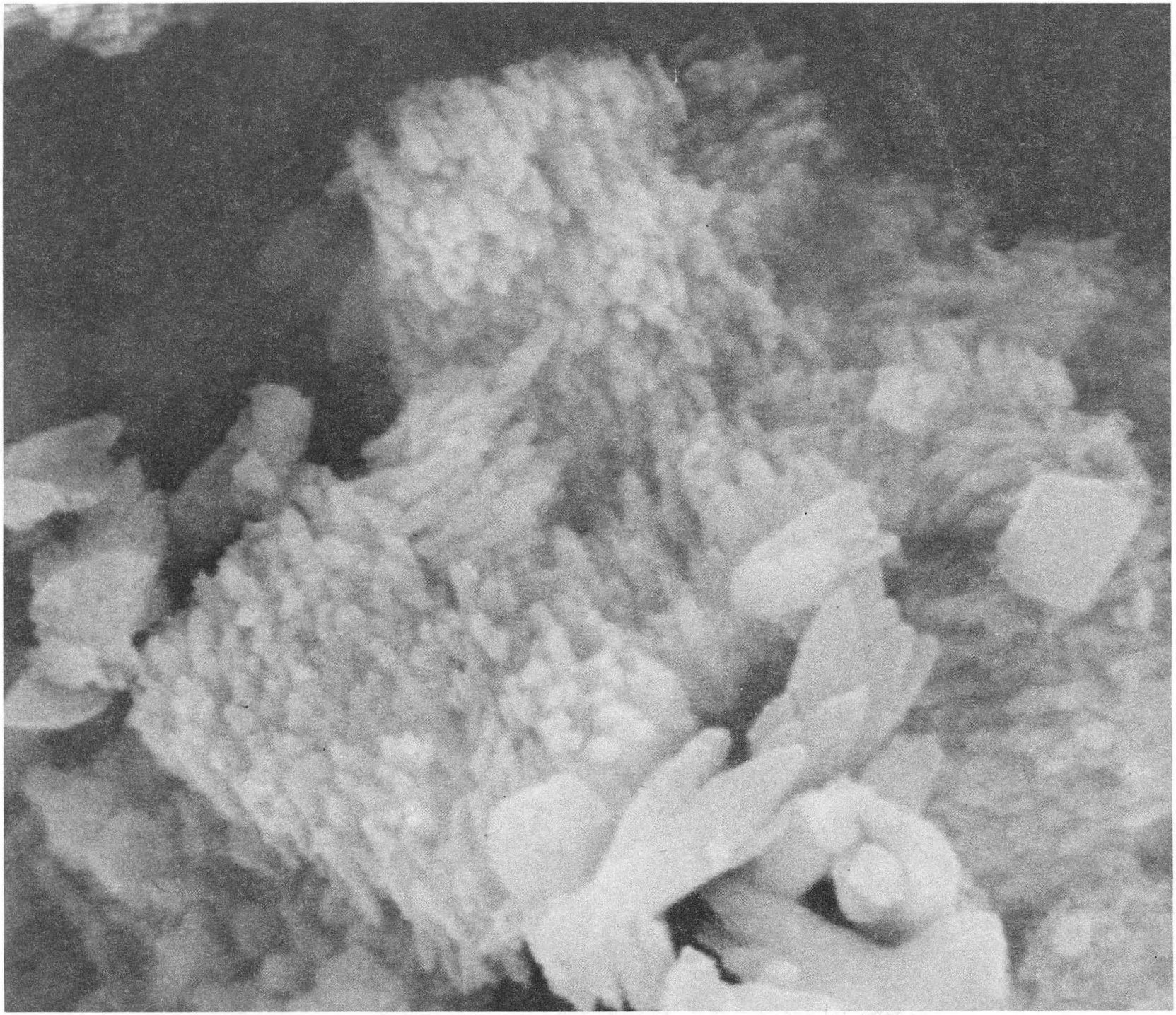

Fig. 4

XBB796 8298

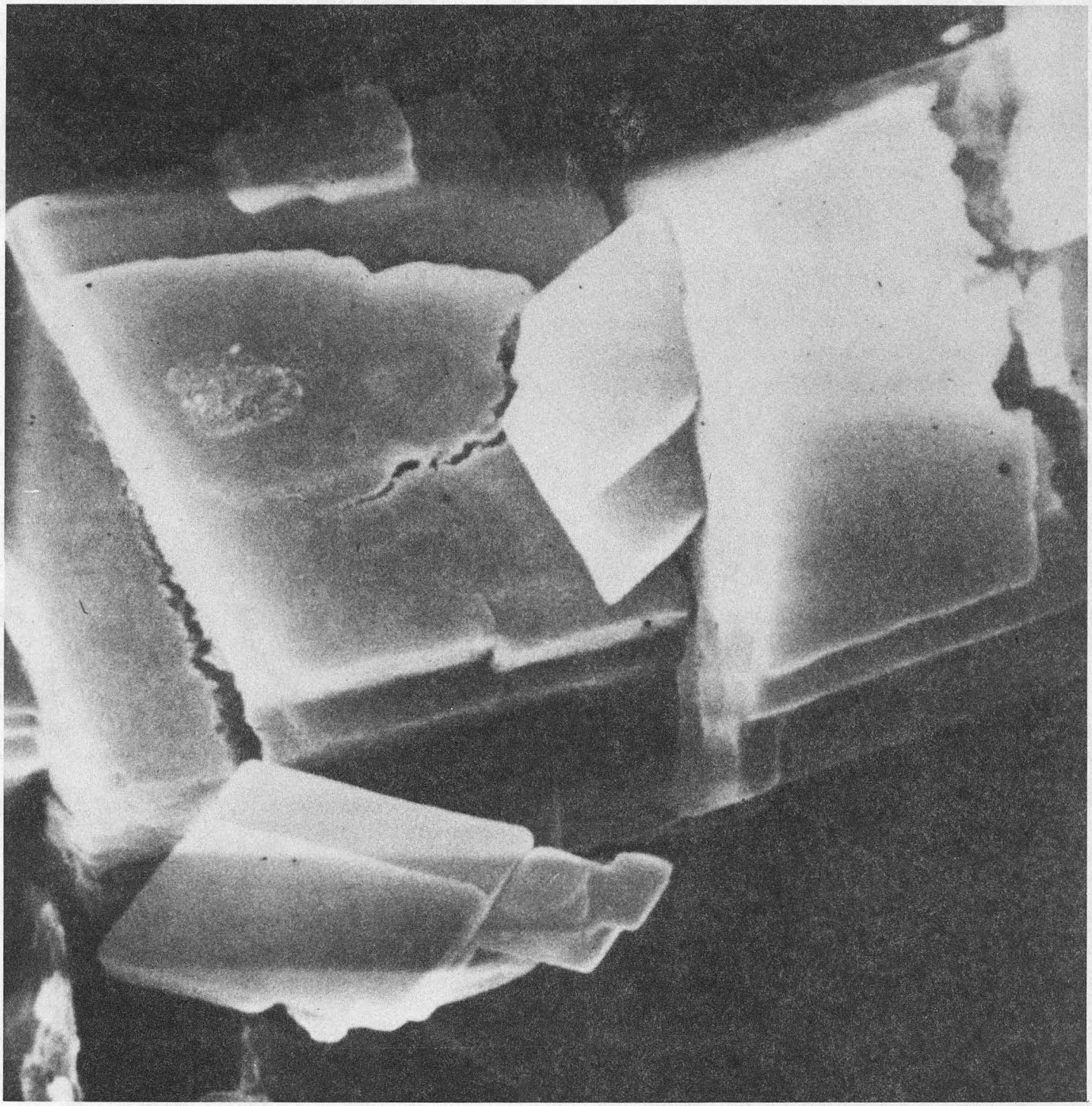

Fig. 5

XBB7912572

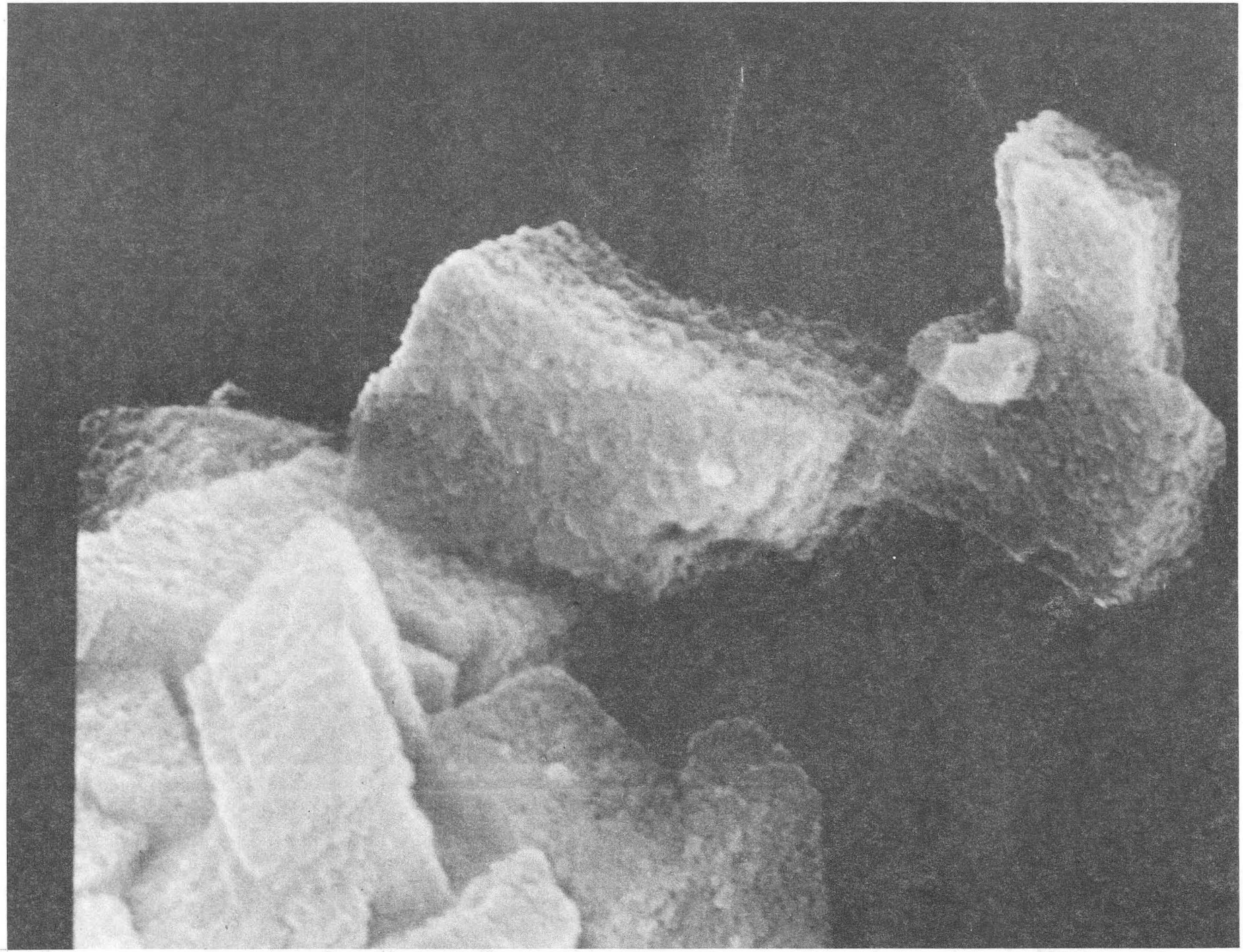

Fig. 6

XBB79912575

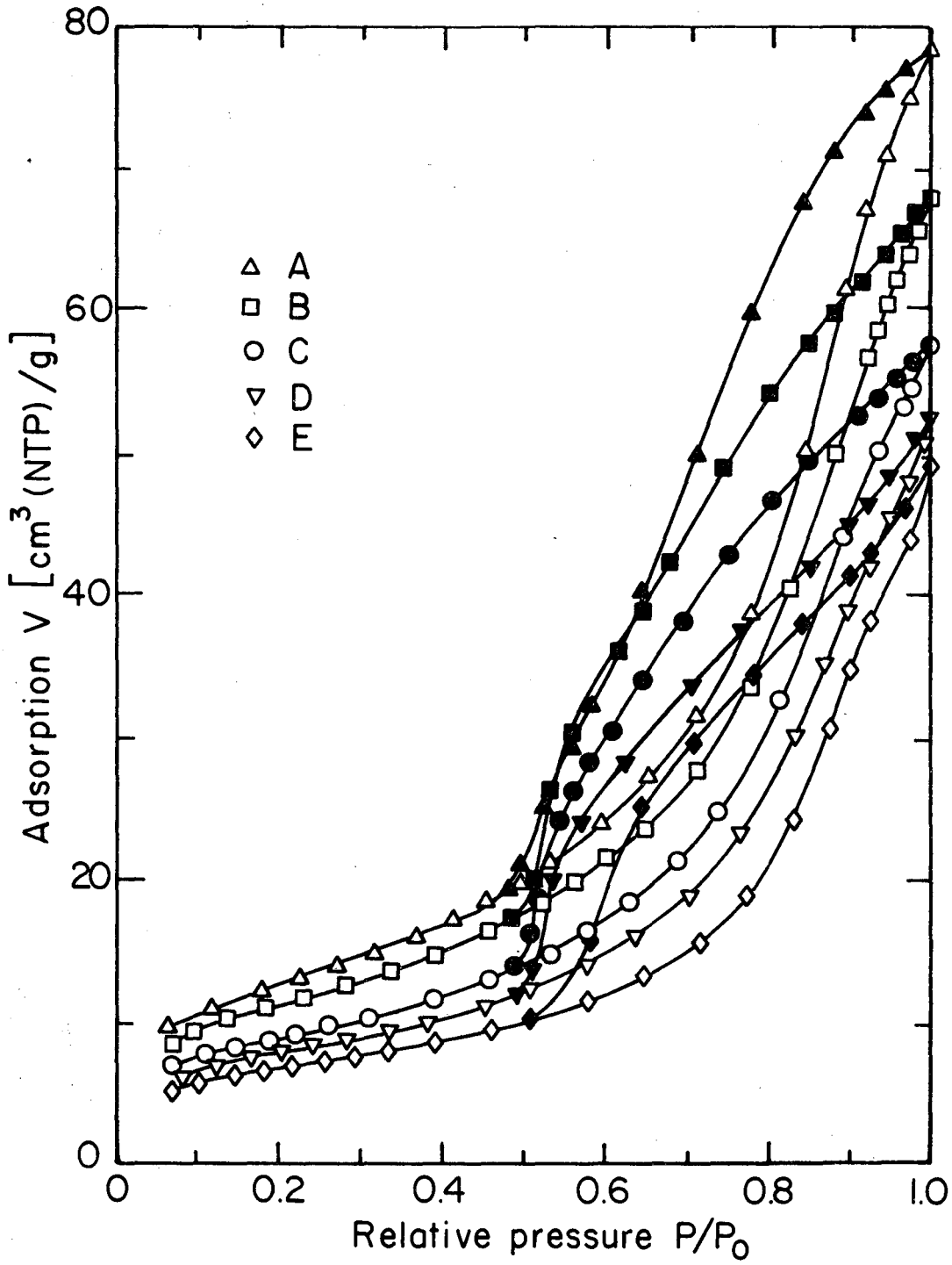

XBL799-7123

Fig. 7

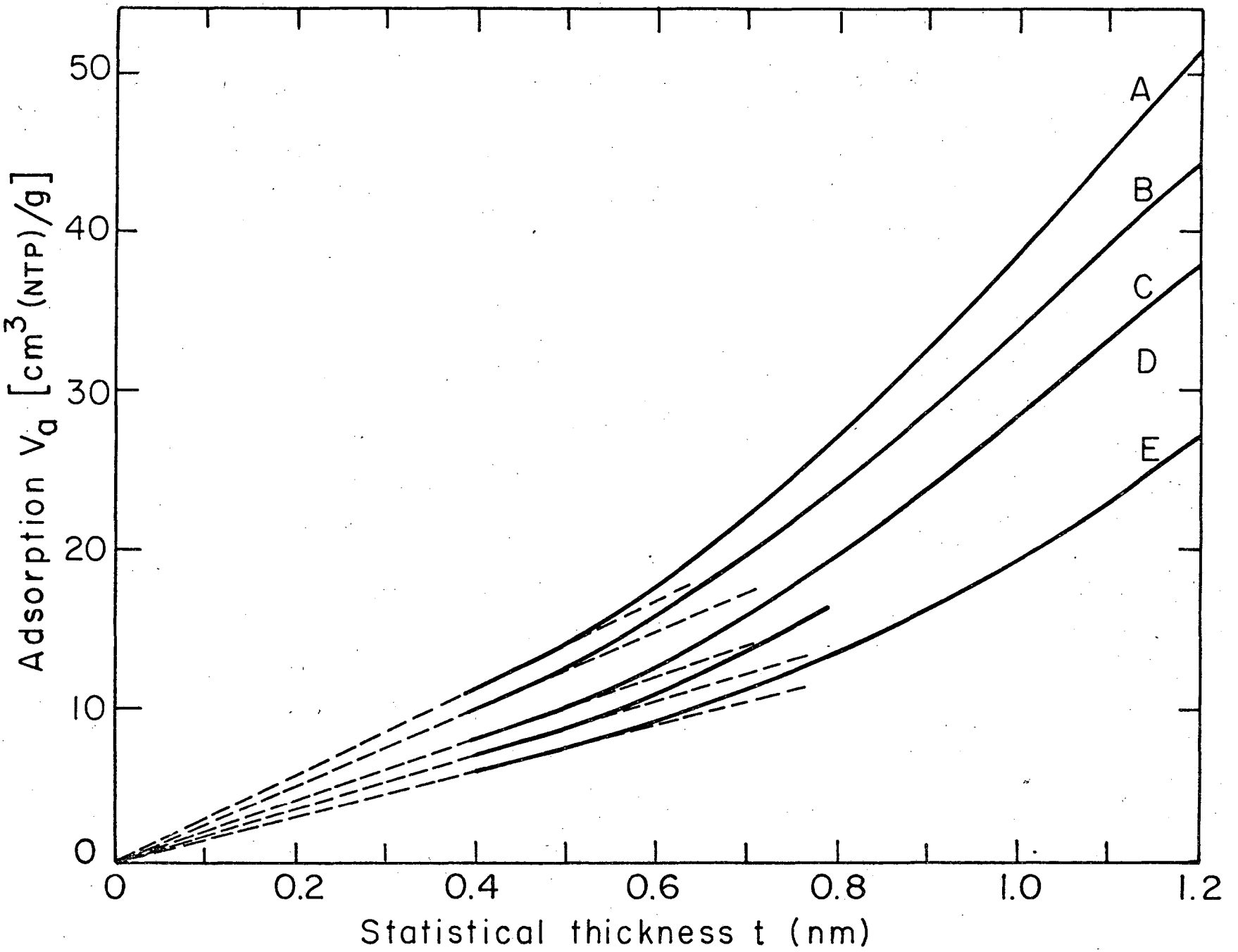

Fig. 8

XBL 806-5277

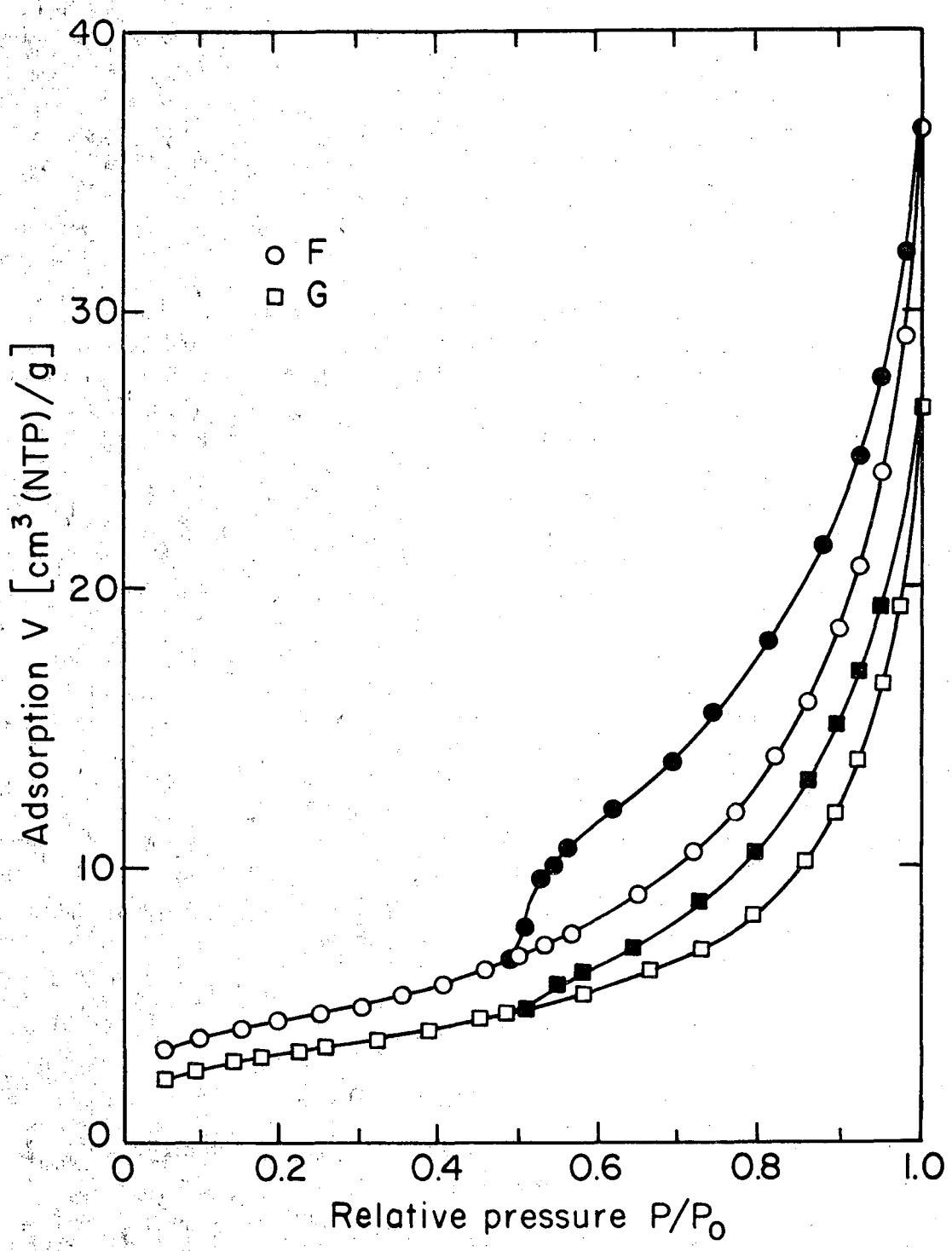

XBL 799-7124

Fig. 9

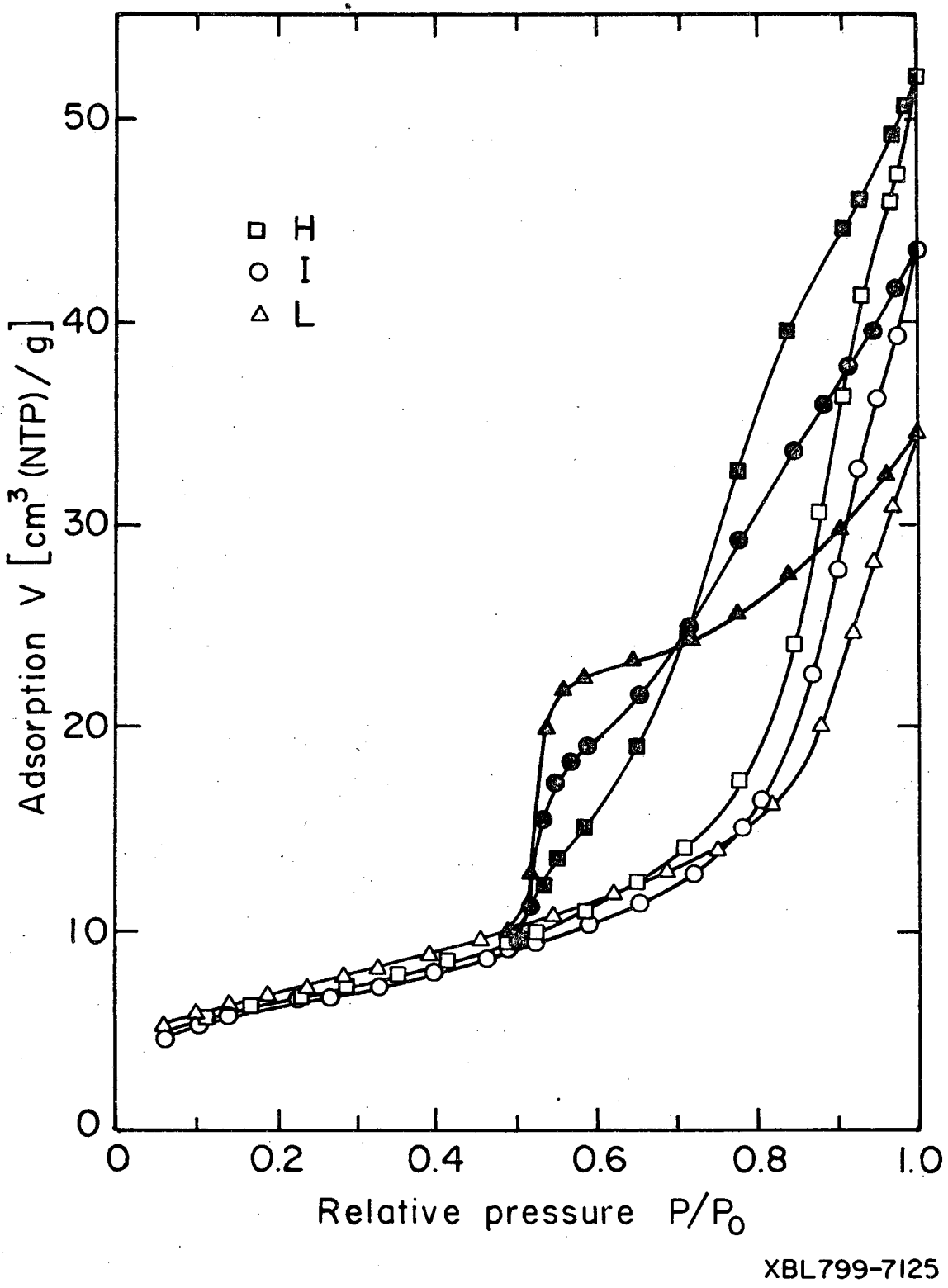
H
I
L
Adsorption V [cm³ (NTP) / g]
0
10
20
30
40
50
0
0.2
0.4
0.6
0.8
1.0
Relative pressure P/P₀
XBL799-7125

Fig. 10

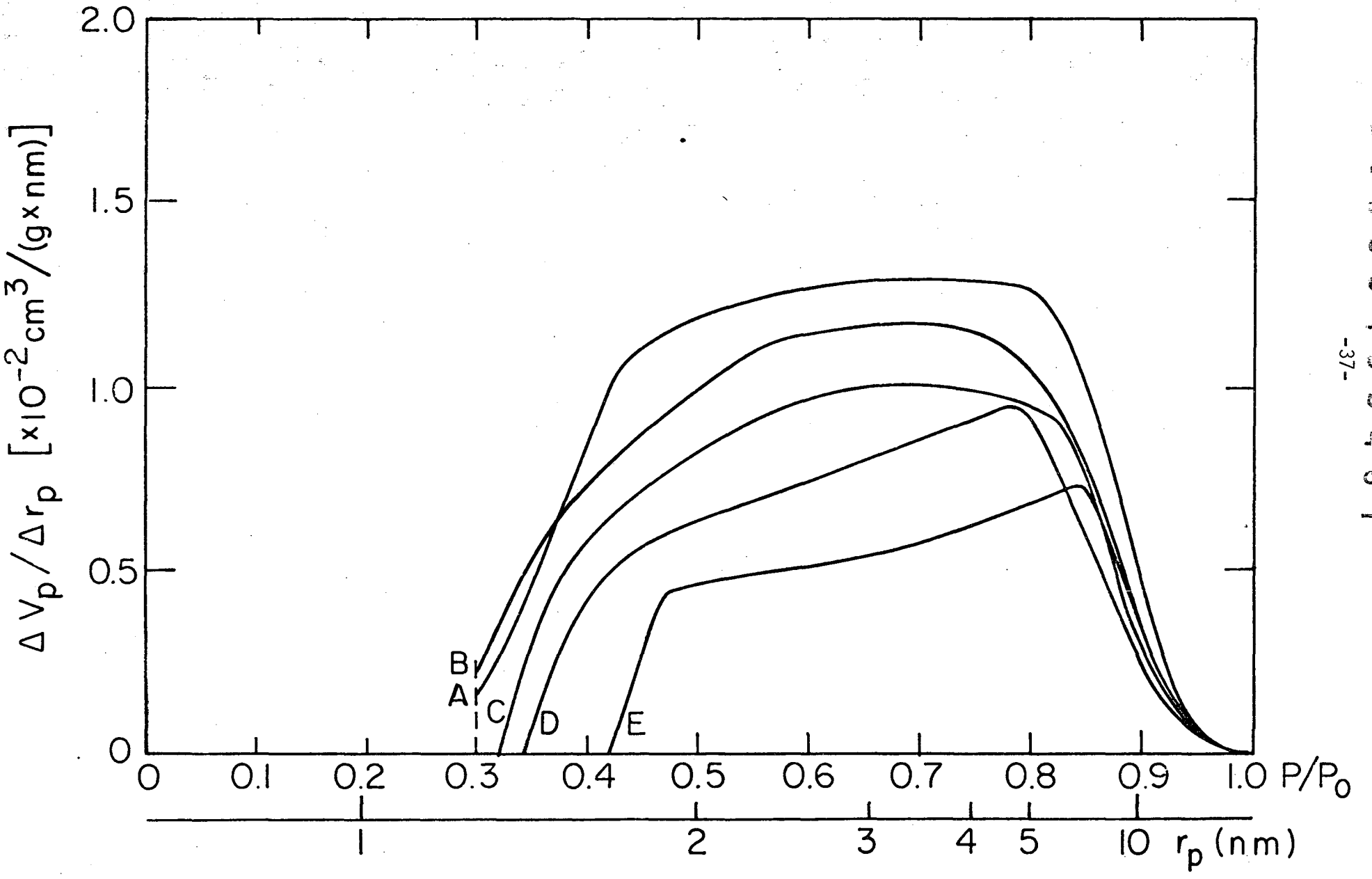

Fig. 11

XBL806-5276

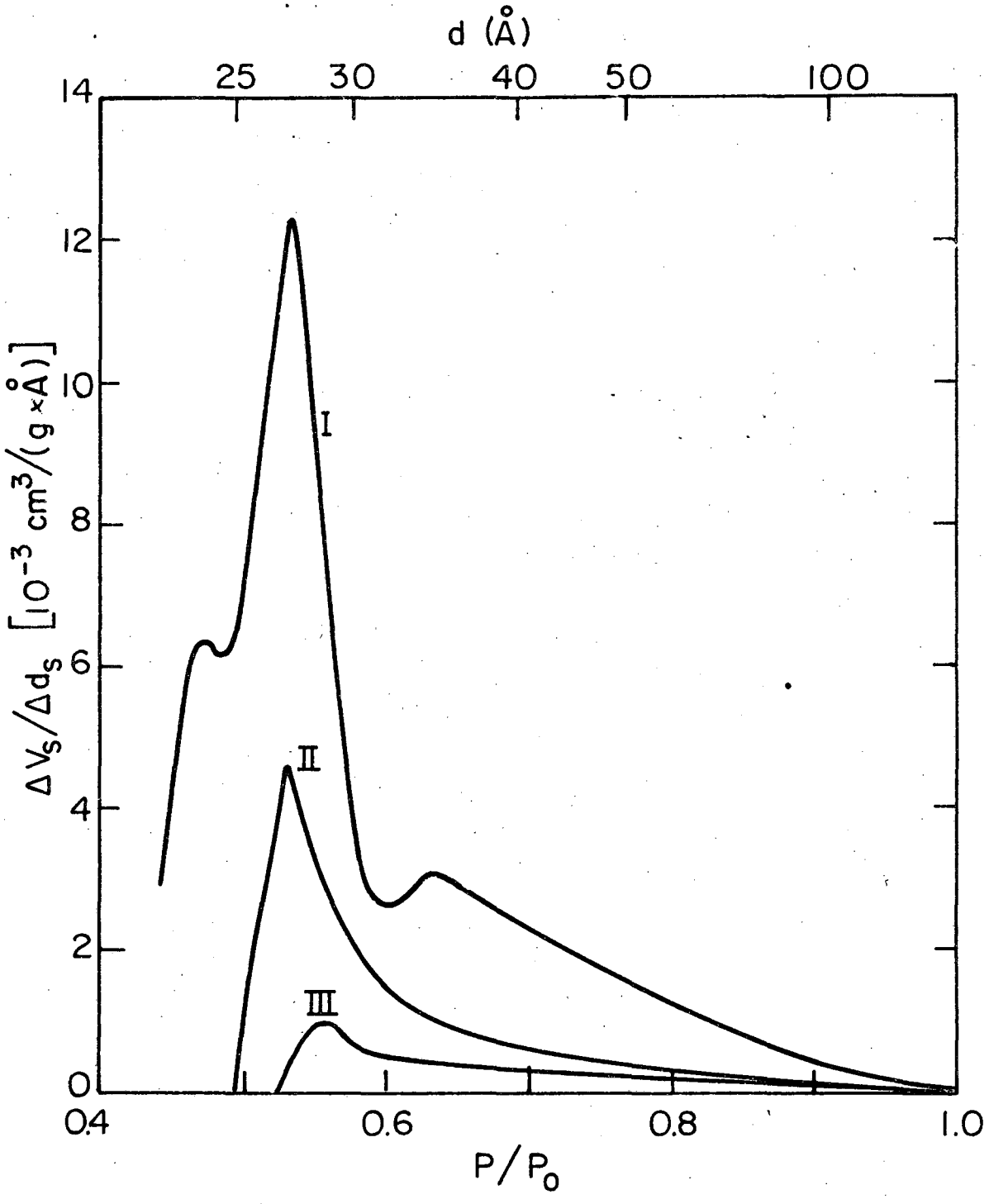

XBL 799-7108

Fig. 12

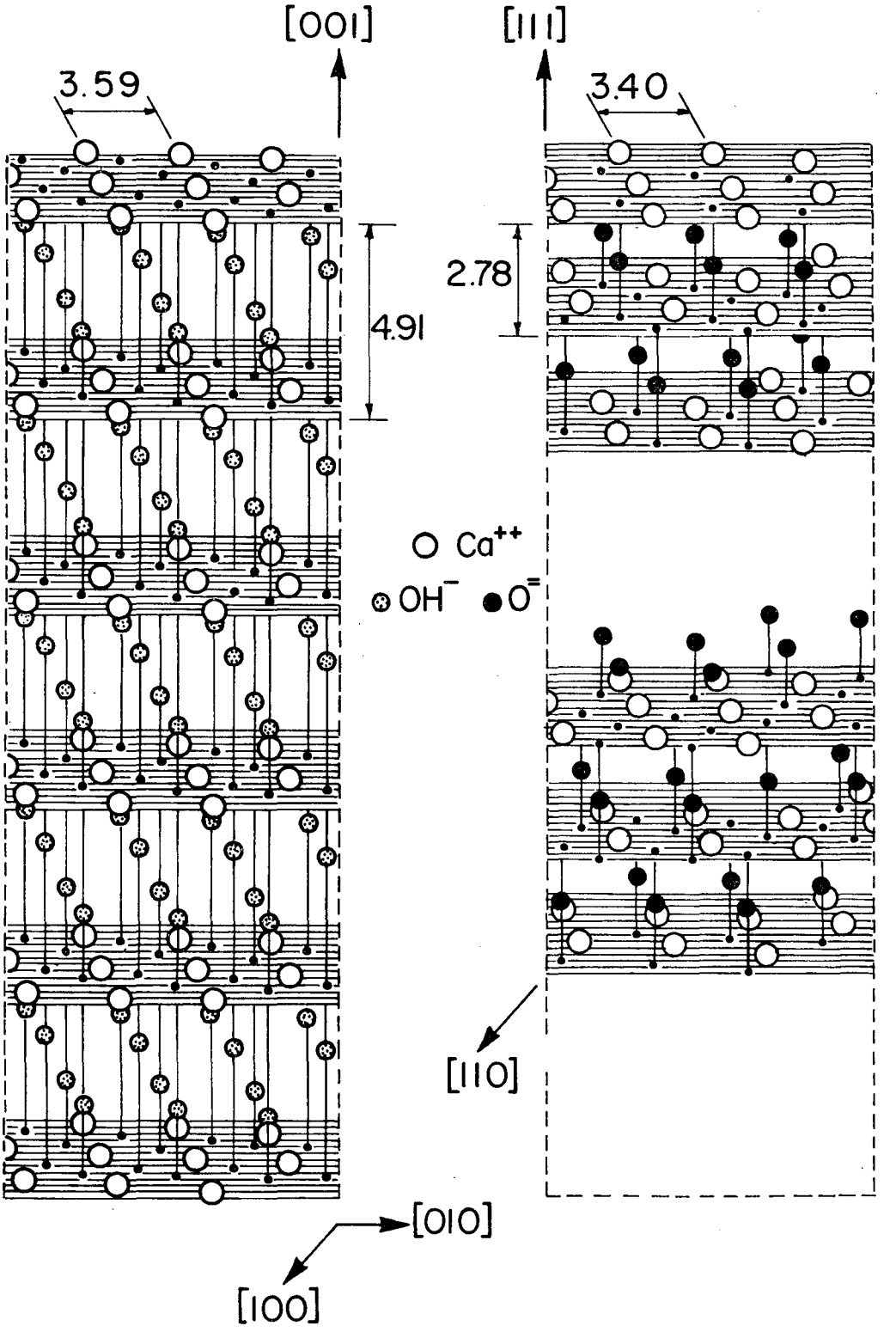

XBL799-7127

Fig. 13

This report was done with support from the Department of Energy. Any conclusions or opinions expressed in this report represent solely those of the author(s) and not necessarily those of The Regents of the University of California, the Lawrence Berkeley Laboratory or the Department of Energy.

Reference to a company or product name does not imply approval or recommendation of the product by the University of California or the U.S. Department of Energy to the exclusion of others that may be suitable.

TECHNICAL INFORMATION DEPARTMENT
LAWRENCE BERKELEY LABORATORY
UNIVERSITY OF CALIFORNIA
BERKELEY, CALIFORNIA 94720